Journal of Science and Transport Technology
Journal homepage: https://jstt.vn/index.php/en

Synthesis and CO gas adsorption properties of GO/$ZnFe_2O_4$ nanocomposites

Vinh Thanh Nguyen[1], Tuan Quoc Tran[1], Cuong Van Nguyen[1], Hung Van Nguyen[2], Hai Thanh Nguyen[2], Hang Thi Bui[2], Dang Van Tran[2], Quy Van Nguyen[2*]

[1]University of Transport Technology, Ha Noi 100000, Viet Nam
[2]International Training Institute for Materials Science, Ha Noi University of Science and Technology, Ha Noi 100000, Viet Nam

Article info
Type of article:
Original research paper

DOI:
https://doi.org/10.58845/jstt.utt.2022.en.2.4.1-8

***Corresponding author:**
E-mail address:
quy@itims.edu.vn

Received: 26/11/2022
Revised: 17/12/2022
Accepted: 19/12/2022

Abstract: In this work, $ZnFe_2O_4$ nanoparticles were synthesized by hydrothermal method while the hummer method was used to synthesize GO nanosheet. GO/$ZnFe_2O_4$ nanocomposites (GO/ZFO) were prepared by mixing GO with $ZnFe_2O_4$ in mass ratio of 1:99, respectively. The structure, morphology, and physical – chemical characteristics were determined by Raman spectroscopy, Transform Electron Microscopy (TEM), and Fourier Transform Infrared Spectroscopy (FT-IR). The CO gas adsorption properties of GO/ZFO were investigated in the range of 25 – 200 ppm at room temperature using quartz crystal microbalance (QCM). GO/ZFO nanocomposites show great adsorption – desorption capacity, high repeatability, and the largest adsorption performance of 1.21‰ (0.098 μg.cm^{-2} at 200 ppm). The results show that this new approach is promising of spinel structure materials for CO adsorption at room temperature.

Keywords: $ZnFe_2O_4$, GO, QCM, CO, Adsorption.

1. Introduction

Carbon monoxide (CO) is one of the most common toxic gases that results from the incomplete burning of fossil fuels. CO is a colorless, odorless and tasteless gas, known as the “silent killer” [1],[2],[3]. In addition, CO is considered as the major gaseous pollutant causing about 40,000 cause of poisoning per year in the United States of American [4]. The industry’s booming together with the increasing number of motor vehicles have led to a dramatically increase in CO emissions which is directly posing a serious threat to human life, work and living environment. Thus, CO treatment, adsorption and detection are researches of great significance to our society.

Recently, quartz crystal microbalance (QCM) coated with sensing materials is used to detect CO gas through physical/chemical adsorption. These studies not only make a great contribution to the development of sensor technology but also give us a comprehensive understanding of the gas adsorption properties [5],[6]. On the other hand, CO adsorption sensitivity studies can be approached by density functional theory. These calculation results indicate that the materials based on graphene can be considered as potential adsorption materials for toxic gases, such as carbon monoxide [7-9]. Furthermore, using the experimental approach, QCM coated with graphene oxide nanosheets (GO NSs) demonstrate a quick response, good repeatability and long-term stability to CO tests at room

temperature [10]. In addition, QCM sensors based on iron oxide/iron oxide-hydroxide and zinc ferrite nanoparticles ($ZnFe_2O_4$ NPs) nanomaterial also show CO detection capacity via physical interaction [11],[12].

From this view point, the combination between GO NSs and $ZnFe_2O_4$ NPs promises an excellent CO adsorbent. Therefore, GO/$ZnFe_2O_4$ nanocomposites were created in this work and our experiments were carried out to understand their CO adsorption characteristics. In the present study, we report new results related to the adsorption capacity, repeatability and adsorption – desorption time of GO/$ZnFe_2O_4$ nanocomposites for CO gas at room temperature in the concentration range of 25 – 200 ppm. These promising results provide an interesting research direction in the near future.

2. Experiment

2.1. GO/$ZnFe_2O_4$ (GO/ZFO) nanocomposites synthesis

Chemicals used in this experiment include: zinc nitrate hexahydrate ($Zn(NO_3)_2.6H_2O$, > 98%), ferric nitrate nonahydrate ($Fe(NO_3)_3.9H_2O$, > 98%), sodium hydroxide (NaOH, > 98%), acid sulfuric (H_2SO_4, 98%), sodium nitrate ($NaNO_3$, > 98%), potassium permanganate ($KMnO_4$, > 98%) and hydrogen peroxide (H_2O_2) supplied from Xilong Scientific Co., Ltd (Guang-dong, China) while flake graphite was bought from VNGraphene Co. (Ha Noi, Viet Nam). The 5 MHz AT-cut quartz crystal microbalance was purchased from Quartz Pro Co (Sweden). Deionized water (DI) was used in all experiment steps.

In order to synthesize GO NSs, a typical process hummer was used, which is really helpful because it is easy to make and produce in large quantities. Furthermore, hummer method provides GO NSs with either hydroxyl, epoxide-rich or more carbonyl-rich [13],[14],[15] while the gas adsorption capacity of nanomaterial has been shown to strongly depend on active functional groups (-OH, -COOH, C-O-C, …) or vacancies, defects.

In this study, the basic steps of hummer method are as follow: (i) a mixture of 0.2 g flake graphite and 0.1 g $NaNO_3$ was added to 16 ml of 98% H_2SO_4. This solution was stirred for 2 hours at room temperature. 0.8 g of $KMnO_4$ was then slowly added for 15 minutes. The reaction released gas and changed the color of solution into brown. This solution was continuously stirred for 48 hours at room temperature. After that, 50 ml of DI was added to dilute the solution. In the next step, an amount of H_2O_2 was slowly dropped into the solution, until the solution's color was completely changed into yellow. The final product was washed and filtered by centrifugation using DI and HCl till the pH reached 7. Additionally, the concentration of GO NSs solution was 1.32 mg/ml.

The synthesis of $ZnFe_2O_4$ nanoparticles (ZFO NPs) via hydrothermal method has already been reported in our previous work. These results indicate that the product of hydrothermal method has high crystallinity, uniform morphology, stability, porosity and large specific surface area. These factors enhance gas adsorption properties [11]. Moreover, 482 mg of ZFO NPs and 3.69 ml of GO NSs solution were dropped into 30 ml of DI, which was quickly mixed using magnetic stirrer for 30 minutes followed by 30 minutes of ultrasonic vibration. This two-steps process was repeated for 4 times. Finally, the as-prepared sample was dried at 60 ^oC for 48 hours. Obtained GO/ZFO composite exhibits the black powder.

2.2. Characteristics

The Raman spectra of GO/ZFO nanocomposites were recorded by Via Micro-Raman Microscope (Renishaw) using the excitation laser wavelength of 633 nm while FT-IR Jasco 4600 spectrophotometer was used to examine the physicochemical of the as-prepared sample in the wavenumber range of 4000 – 400 cm^{-1}. The morphology of GO/ZFO nanocomposites was observed by Transmission Electron Microscopy (TEM, JOEL 1010).

2.3. Gas adsorption properties test

In order to fabricate QCM sensor, an AT-cut 5 MHz QCM was washed by ethanol and dried by N_2 flow. Then, 80.72 µg.cm^{-2} of the GO/ZFO mass density (Δm_o) was coated on the QCM's active electrode by spray-coating method. The coating process has been described in details in the previous works [16]. The gas adsorption properties of GO/ZFO nanocomposites (including: adsorption – desorption, repeatability and adsorption performance) were assessed through the change of mass density on the QCM's electrode (*Δm, µg/cm^2*) and the CO sorption capacity per unit mass density of material sensing (*S, ‰)* [17], respectively. In which, the CO molecules are continuously adsorbed/desorbed by GO/ZFO during the test experiments causing *Δm,* and *Δm* is determined by Sauerbrey's formula [18]:

$$\Delta m = -\frac{\Delta f}{C_f} \quad (1)$$

where Δf is frequency shift or response of QCM sensor in Hz; C_f = *56.6 Hz cm^2/µg^1* is sensitive factor. Furthermore, the repeatability of material sensing is visually recognized by relative error (*R-error* in *%*), which can be calculated as followed [16]:

$$R-error = \frac{|\Delta m_1 - \Delta m_n|}{\Delta m_1}.100 \quad (2)$$

Δm_1 & Δm_n are CO mass densities absorbed on GO/ZFO sensing layer at the first and n^{th} cycle of the sensor. Additionally, *S* of GO/ZFO was determined by formula (3):

$$S = \frac{\Delta m}{\Delta m_o}.1000 \quad (3)$$

In addition, limit of detection (*LOD*, ppm), one of the important factors, is determined by formula (4):

$$LOD = \frac{3S_b}{S} \quad (4)$$

S_b is the standard deviation of the response and *S* is the rope of the calibration curve [19].

3. Results and Discussion

Fig.1 shows the characteristics of the as-prepared GO/ZFO nanocomposites powder. The three main peaks at around 353, 508, and 660 cm^{-1} can be clearly observed in Raman spectra, as depicted in Fig. 1a, which correspond to the three first-order modes (F_{2g} (2), F_{2g}(3) and A_{1g}) of $ZnFe_2O_4$ NPs, respectively [20],[21],[22]. Moreover, two strong peaks at 1314 cm^{-1} and 1588 cm^{-1} are known as D band and G band of GO NSs, respectively. Thus, these characteristic peaks confirm that GO NSs and $ZnFe_2O_4$ NPs are component of GO/ZFO nanocomposites [23]. Fig. 1b illustrates the FT-IR spectra of GO/ZFO. It clearly shows that the adsorption peak at 3407 cm^{-1} corresponds to the stretching vibration of O-H and H-O-H, while the strongest peaks in the range of 1350 – 1650 cm^{-1} represent the important bindings of GO NSs, such as: C=C (1645 cm^{-1}) and C-O (1381 cm^{-1}) [24],[25]. Moreover, ferrite often has metallic-oxygen bonds at 555 and 414 cm^{-1}, which were assigned to the bonds at tetrahedral site (M_{tetra} – O) and octahedral site (M_{octa} – O) of ZFO cubic structure, respectively [26]. The sample's morphology was disclosed by TEM image (Fig. 1c). It shows that the small cubic particles are the main shapes of ZFO in this sample, these particles size ranges from 6 to 30 nm. On the other hand, the pale plates on the cubic particles are assigned to GO NSs. Thus, these results in Fig.1 indicate that GO/ZFO nanocomposites were successfully synthesized.

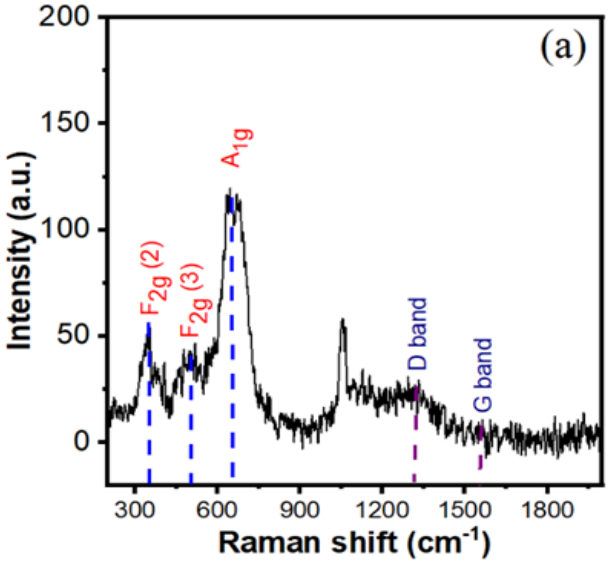

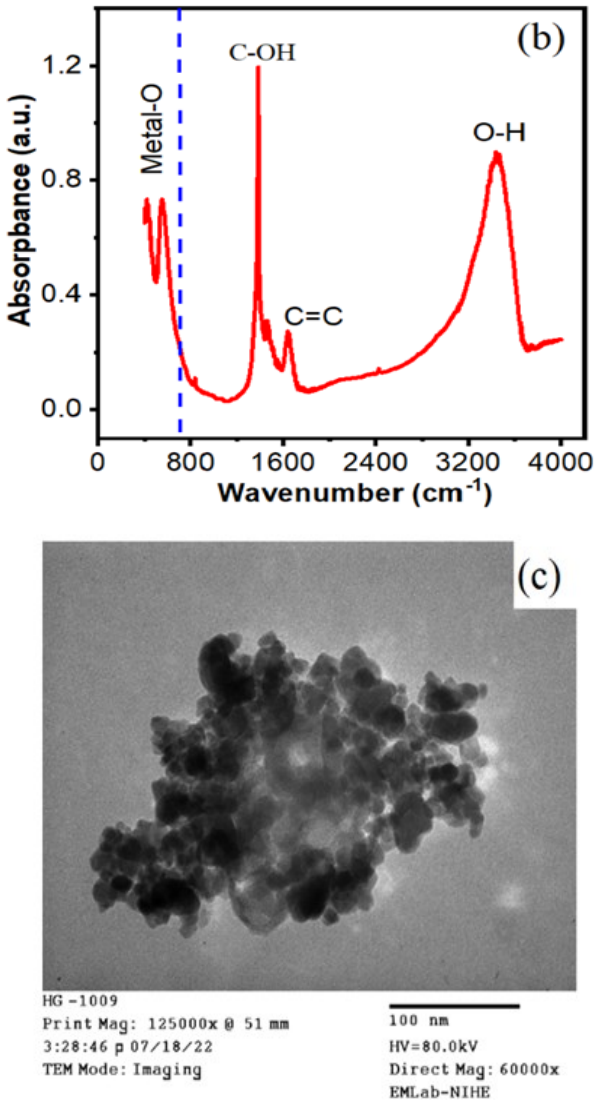

Fig. 1. (a) Raman, (b) FT-IR and (c) TEM of GO/ZFO

The CO adsorption/desorption kinetics were investigated under a large concentration range of 25 – 200 ppm at room temperature using QCM. There were two stages for each cycle test. In the first stage, CO/N_2 gas mixture was blown into the testing gas chamber. The mass on the active electrode increased because GO/ZFO sensing layer tended to adsorb CO molecules, QCM sensor responded by reducing the resonant frequency. In the second stage, CO molecules were removed by N_2 gas flow, causing a mass decrease on the QCM's electrode and an increase in resonance frequency simultaneously. The response of QCM sensor is frequency shift, using equation (1) to calculate the absorbed CO mass density. Fig. 2a shows adsorption – desorption curve for five CO expose cycles of the sensor. In other words, the change of mass density is determined by the Δm difference between the two times "CO in" and "CO out" for each cycle, as shown Fig. 2a. Moreover, it could be observed that the adsorbed mass density significantly increases with the increasing of CO concentration. Namely, the change of mass densities on the QCM's electrode was 0.005/0.010/0.034/0.069/0.098 $\mu g.cm^{-2}$ at 25/50/100/150/200 ppm, respectively.

The adsorption performance was calculated by formula (3), which are 0.06‰ (25 ppm), 0.12‰ (50 ppm, 0.42‰ (100 ppm), 0.85‰ (150 ppm) and 1.21‰ (200 ppm). In this case, the maximum experiment test is 200 ppm (ppm is mean parts per million) which is converted to 229.122 µg/l, and this is very small concentration. Furthermore, at this concentration, the adsorption performance is 1.21‰, that means 1000 µg of GO/ZFO nanocomposites can absorb 1.21 µg CO ($\sim 2.6 \times 10^{16}$ CO molecules) per a square centimeter. This is a big number in the micro world. Additionally, the change values of mass density are illustrated in Fig. 2b and the adsorption performance results are compared to some references and summarized in Table. 1. The CO adsorption performance of GO/ZFO nanocomposites is linearly proportional to CO concentration in the range of 25 – 200 ppm, the correlation coefficient (R^2) is 0.98904. The high value of R^2 represents the fit of linear model between CO adsorption performance and CO concentration. From the data in Fig. 2b, S and S_b were calculated and had values of 5.924×10^{-4} and 3.864×10^{-3}, respectively. Using equation (4), *LOD* was calculated to have value of 19.57 ppm. Moreover, the short averaging times of CO exposure are recommended (remain valid) by World Health Organization (WHO), these values are 30.55 ppm (30 mg/m^3) and 87.29 ppm (100 mg/m^3) for 1 hour and 15 minutes, respectively [1]. Thus, the *LOD* of this research represents a great meaning because GO/ZFO nanocomposites can

self-adsorb CO under the recommended level.

In order to examine the repeatability, the GO/ZFO sensor was exposed at 150 ppm for four cycles. It is clear that the curves are identical at all periods. The results demonstrate that the adsorption-desorption process is good reversible, as observed in Fig. 3. The average change of mass density is 0.071 μg/cm^{-2} and the relative error is determined by equation (2) that is 4.2%. Therefore, GO/ZFO nanocomposites show high repeatability adsorption/desorption at room temperature.

Fig. 4 describes the adsorption kinetics of GO/ZFO when this sensor is exposed to 150 ppm CO. The mass density of CO was adsorbed to the saturation in 679 s while desorption time is only 337 s, and the change of mass density is 0.071 μg/cm^2. Moreover, the adsorption/desorption rate is 0.1046/0.2107 ng/(cm^2 s), respectively. It is clear that desorption rate is approximately twice as much as the adsorption rate. The adsorption mechanism of GO/ZFO sensing layer toward CO gas is based on the interaction between active groups on the surface of GO/ZFO and CO molecules via hydrogen bond [10].

Table 1. Comparison between this work and reported researches

Sensing material	*Con. (ppm)*	*S-factor (Hz/ppm)*	*S (‰)*	References
Iron doped six calix[4]arene	-	0.0024	-	[6]
Ferrocene	0-2000	0.0036	-	
Chitosan	0-2000	0.0373	-	[5]
Ferrocene-Chitosan	0-2000	0.0544	-	
GO NSs	150	0.0613	-	[10]
Fe_3O_4/FeOOH	150	0.0560	-	[12]
GO/ZFO nanocomposites	200	0.0369*	1.21	This work

* Using formula: *S-factor* = *(C_f*Δm/Con.)*

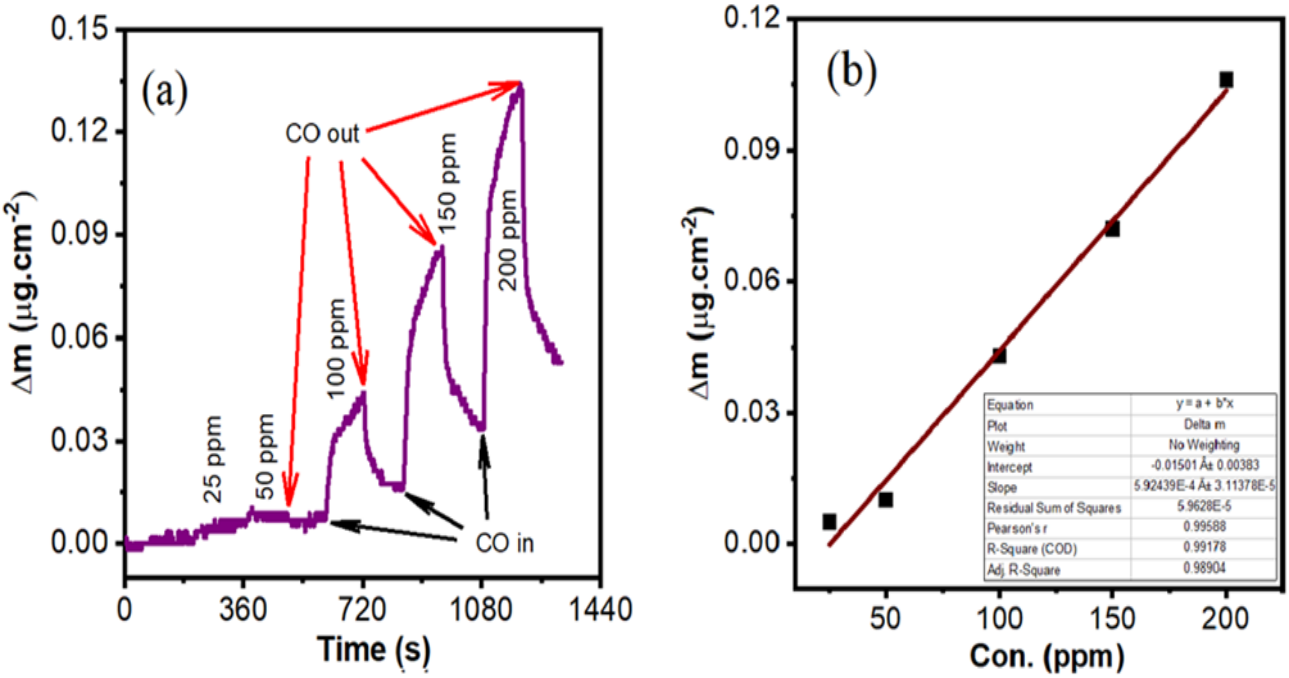

Fig. 2. (a) The adsorption – desorption curves of GO/ZFO sensor and (b) the relationship between sensor adsorption performance and CO concentrations

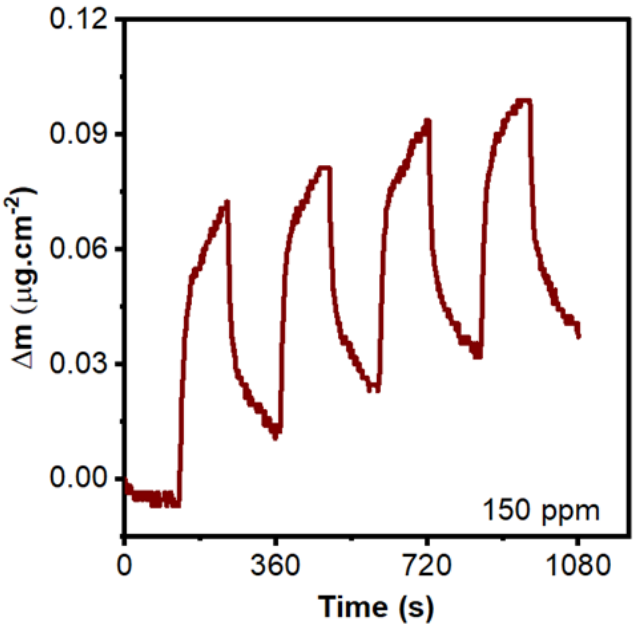

Fig. 3. The repeatability of GO/ZFO sensor at 150 ppm CO

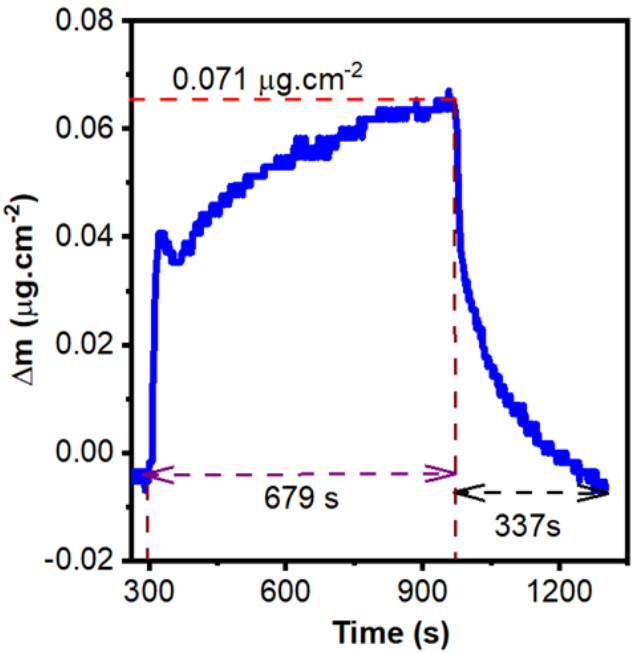

Fig. 4. The saturation adsorption curve of GO/ZFO sensor at 150 ppm CO

4. Conclusion

In summary, the GO/$ZnFe_2O_4$ nanocomposites were successfully synthesized and CO adsorption performance was tested by using QCM. The as-prepared material indicates the excellent CO adsorption properties at room temperature, such as: the maximum of adsorption performance is 1.21‰ at 200 ppm; high linear proportional adsorption performance according to target gas concentration (R^2 = *0.98904*); great repeatability for four cycles with low relative error (*R-error = 4.2%);* low limit of detection (*LOD = 19.57 ppm*) and fast saturation as well as adsorption/desorption. These results are unwavering premises for the development of reusable CO adsorption material systems in the coming future.

Acknowledgments

This research is funded by Hanoi University of Science and Technology (HUST) under project number T2022-TĐ-004.

References

[1] The Lancet. (2006). WHO's global air-quality guidelines. *Lancet*, 368(9544), 1302.

[2] L.J. Wilkinson. (2007). Carbon monoxide - The silent killer. Mol. Death, Second Ed, pp 37-47.

[3] I. Blumenthal and M. Dch. (2001). Carbon monoxide poisoning. *Journal of the Royal Society of Medicine*, 94(6), 270-272.

[4] G. Reumuth, Z. Alharbi, K.S. Houschyar, B.-S. Kim, F. Siemers, P.C. Fuchs, G. Grieb. (2019). Carbon monoxide intoxication: What we know. *Burns*, 45(3), 526-530.

[5] A. Bayram, C. Özbek, M. Şenel and S. Okur. (2017). CO gas sorption properties of ferrocene branched chitosan derivatives. *Sensors and Actuators B: Chemical*, 241, 308-313.

[6] C. Özbek, S. Okur, Ö. Mermer, M. Kurt, S. Sayin, and M. Yilmaz. (2015). Effect of Fe doping on the CO gas sensing of functional calixarene molecules measured with quartz crystal microbalance technique. *Sensors and Actuators B: Chemical*, 215, 464-470.

[7] Y. Zheng, E. Li, C. Liu, K. Bai, Z. Cui, and D. Ma. (2021). Adsorbed of toxic gas molecules (CO, H_2S, and NO) on alkali-metal-doped g-GaN monolayer. *Journal of Physics and Chemistry of Solids*, 152, 109857.

[8] Y. Tang, Z. Liu, Z. Shen, W. Chen, D. Ma, and X. Dai. (2017). Adsorption sensitivity of metal atom decorated bilayer graphene toward toxic

gas molecules (CO, NO, SO_2 and HCN). *Sensors and Actuators B: Chemical*, 238, 182-195.

[9] Z. Gao, Y. Sun, M. Li, W. Yang, and X. Ding. (2018). Adsorption sensitivity of Fe decorated different graphene supports toward toxic gas molecules (CO and NO). *Applied Surface Science*, 456, 351-359.

[10] V.V. Cat, N.X. DInh, V.N. Phan, L.A. Tuan, M.H. Nam, V.D. Lam, T.V. Dang, N.V. Quy. (2020). Realization of graphene oxide nanosheets as a potential mass-type gas sensor for detecting NO_2, SO_2, CO, and NH_3. *Materials Today Communications*, 25, 101682.

[11] N.T. Vinh, N.T. Hai, T.V. Dang, B.T. Hang, A.-T. Le, T.N. Pham, N.X. Dinh, V.D. Lam, M.H. Nam, T.D. Thanh, N.T. Huy, N.V. Quy. (2021). Dual-functional sensing properties of $ZnFe_2O_4$ nanoparticles for detection of the chloramphenicol antibiotic and sulphur dioxide gas. *Sensors and Actuators A: Physical*, 332, 113093.

[12] N. T. Vinh, L. A. Tuan, L. K. Vinh, and N. Van Quy. (2020). Synthesis, characterization, and gas sensing properties of Fe_3O_4/FeOOH nanocomposites for a mass-type gas sensor. *Materials Science in Semiconductor Processing*, 118(5), 105211.

[13] J. Aixart, F. Díaz, J. Llorca, and J. Rosell-Llompart. (2021). Increasing reaction time in Hummers' method towards well exfoliated graphene oxide of low oxidation degree. *Ceramics International*, 47(15), 22130-22137.

[14] T. Munir, M. Imran, S. Muzammil, A.A. Hussain, M. Fakhar-e Alam, A. Mahmood, A. Sohail, M. Atif, S. Shafeeq, M. Afzal. (2022). Antimicrobial activities of polyethylene glycol and citric acid coated graphene oxide-NPs synthesized via Hummer's method. *Arabian Journal of Chemistry*, 15(9), 104075.

[15] P.P. Brisebois and M. Siaj. (2019). Harvesting graphene oxide – years 1859 to 2019: a review of its structure, synthesis, properties and exfoliation. Journal of *Materials Chemistry C*, 8(5), 1517-1547.

[16] N.T. Vinh, T.V. Dang, B.T. Hang, T.T. Loan, A.-T. Le, N.V. Quy. (2022). Synthesis and Gas Adsorption Properties of γ-Fe_2O_3 Nanoparticles for Mass-Type Sensing Application. *Particle & Particle Systems Characterization*, 39(8), 2200063.

[17] M. Matsuguchi, K. Tamai, and Y. Sakai. (2001). SO_2 gas sensors using polymers with different amino groups. *Sensors and Actuators B: Chemical*, 77(1-2), 363-367.

[18] G. Sauerbrey. (1959). Verwendung von Schwingquarzen zur Wagung dünner Schichten und zur Mikrowagung. Zeitschrift für Physik, 155(2), 206-222.

[19] A. Shrivastava and V.B. Gupta. (2011). Methods for the determination of limit of detection and limit of quantitation of the analytical methods. *Chronicles of Young Scientists*, 2(1), 21-25.

[20] N.N. Huyen, N.T. Anh, T.L.H. Phung, N.X. Dinh, N.T. Vinh, T.T. Loan, V.Q. Nguyen, D.L. Vu, L.M. Tung and A.-T. Le. (2022). Boosting the Selective Electrochemical Signals for Simultaneous Determination of Chloramphenicol and Furazolidone in Food Samples by Using $ZnFe_2O_4$-Based Sensing Platform: Correlation between Analyte Molecular Structure and Electronic Property of Electrode Materials. *Journal of the Electrochemical Society*, 169(10), 106517.

[21] N.T. Anh, N.N. Huyen, N.X. Dinh, L.K. Vinh, L.M. Tung, N.T. Vinh, N.V. Quý, V. D. Lam and A.-T. Le. (2022). ZnO/$ZnFe_2O_4$ nanocomposite-based electrochemical nanosensors for the detection of furazolidone in pork and shrimp samples: exploring the role of crystallinity, phase ratio, and heterojunction formation. *New Journal of Chemistry*, 46(15), 7090-7102.

[22] Z. Wang, D. Schiferl, Y. Zhao, and H.S.C. O'Neill. (2003). High pressure Raman spectroscopy of spinel-type ferrite $ZnFe_2O_4$.

Journal of Physics and Chemistry of Solids, 64(12), 2517-2523.

[23] Y. Dai, T. Yan, Y. Shi, R. Hong, C. Tao, H. Lin, Q. Wang, D. Zhang. (2021). Tunable surface enhanced Raman scattering of silver thin films by the graphene oxide. *Physica E: Low-Dimensional Systems and Nanostructures*, 130, 114696.

[24] W. Ma, R. Yang, Z. Yang, C. Duan, and T. Wang. (2019). Synthesis of reduced graphene oxide/zinc ferrite/nickel nanohybrids: as a lightweight and high-performance microwave absorber in the low frequency. *Journal of* Materials Science: Materials in Electronics, 30(20), 18496-18505.

[25] M.L. Baynosa, A.H. Mady, V.Q. Nguyen, D.R. Kumar, M.S. Sayed, D. Tuma, J.-J. Shim. (2020). Eco-friendly synthesis of recyclable mesoporous zinc ferrite@reduced graphene oxide nanocomposite for efficient photocatalytic dye degradation under solar radiation. *Journal of Colloid and Interface Science*, 561, 459-469.

[26] P.A. Vinosha, A. Manikandan, R. Ragu, A. Dinesh, P. Paulraj, Y. Slimani, M.A. Almessiere, A. Baykal, J. Madhavan, B. Xavier, G.F. Nirmala. (2021). Exploring the influence of varying pH on structural, electro-optical, magnetic and photo-Fenton properties of mesoporous $ZnFe_2O_4$ nanocrystals. *Environmental Pollution*, 272, 115983.